A new type of size effect in the conductivity of quantized metal films

2002 J. Phys.: Condens. Matter 14 4287

(http://iopscience.iop.org/0953-8984/14/17/302)

INSTITUTE OF PHYSICS PUBLISHING JOURNAL OF PHYSICS: CONDENSED MATTER

J. Phys.: Condens. Matter **14** (2002) 4287–4295 PII: S0953-8984(02)29856-2

A new type of size effect in the conductivity of quantized metal films

A E Meyerovich and I V Ponomarev[1]

Department of Physics, University of Rhode Island, Kingston, RI 02881-0817, USA

E-mail: ilya@uri.edu (I V Ponomarev)

Received 18 October 2001, in final form 11 February 2002
Published 18 April 2002
Online at stacks.iop.org/JPhysCM/14/4287

Abstract

A new type of quantum-size effect (QSE) is predicted for films with a large correlation radius of thickness fluctuations. The large-period oscillations of conductivity σ as a function of thickness L replace the usual QSE for random inhomogeneities with Gaussian and exponential power spectra. A simple quasiclassical picture and an exact quantum explanation are given. The positions of peaks are obtained analytically. High sensitivity of the underlying strong coupling of low quantum well states to thickness fluctuations is inherent to other types of film as well.

Progress in nanofabrication has rekindled interest in studies of quantum well (QW) states in ultrathin metal films exhibiting a quantum-size effect (QSE). Recent QW experiments on quantized metal films include conductivity [1], spectroscopy [2], susceptibility [3], and STM [4] measurements. The QSE is caused by quantization of particle motion in a film, $p_x \to \pi j/L$ (below $\hbar = 1$), and splits the 3D energy spectrum $\epsilon(\boldsymbol{p})$ into a set of minibands $\epsilon_j(\boldsymbol{q})$ ($\boldsymbol{q}$ is the 2D momentum along the film). Experimentally, the linewidth of QW states is often limited by the thickness fluctuations [5]. Below we demonstrate that thickness fluctuations with a large correlation radius lead to a peculiar coupling between QW states with low quantum numbers. As one of the observable consequences, we predict a new type of QSE oscillation in the conductivity of metal films. This opens the way to the observation of the QSE in metal films in which the usual QSE is suppressed. This could also resolve the long-standing controversy regarding the influence of the structure of a nanoscale film on its resistivity [6] and explain the large period of QSE oscillations in some experiments [1].

The form of the correlation function for thickness fluctuations $\zeta(s)$ is routinely identified in surface scattering experiments. However, there has been no comprehensive experimental or theoretical study of the effect of the shape of $\zeta(s)$ on QW states inside the films. We performed such a study for the conductivity of quantized metal films. The most striking result

[1] Author to whom any correspondence should be addressed.

is the new QSE described in this paper. The results can help in the extraction of $\zeta(s)$ and the correlation radius R from conductivity measurements when R is relatively large. We compared $\sigma(L)$ for various types of correlation function identified in scattering experiments and used in calculations [7, 8]: the Gaussian correlator,

$$\zeta(s) = \ell^2 \exp(-s^2/2R^2), \tag{1}$$

power-law correlators with various values of μ,

$$\zeta(s) = 2\mu\ell^2[R^2/(s^2 + R^2)]^{1+\mu}, \tag{2}$$

including the Staras correlator $\mu = 1$, the Lorentzian

$$\zeta(s) = 2\ell^2 R^2/(s^2 + R^2), \tag{3}$$

and correlators with a power-law Fourier image,

$$\zeta(q) = 2\pi\ell^2 R^2/(1 + q^2R^2)^{1+\lambda}. \tag{4}$$

The last group includes the Lorentzian correlator in momentum space, $\lambda = 0$, and the exponential correlator $\zeta(s) = \ell^2 \exp(-s/R)$ at $\lambda = \frac{1}{2}$. All the correlators describe thickness fluctuations of the same average amplitude ℓ and, except for (3), lead to the same conductivity σ in the long-wavelength limit $R/\lambda_F \to 0$ in which σ should not depend on details of the inhomogeneities. The Lorentzian (3) has a logarithmically divergent power spectrum and is often considered 'unphysical'. We added this correlator because it is used in calculations. To deal with the divergency, one can truncate (3) at large distances (commonly, at about a tenth of the system length [7]). (Sometimes, the divergence of $\zeta(q)$ is associated with a fractal nature of the surface; to what extent our approach can be used for films with fractal surfaces is unclear.)

In all four figures, curve 1 corresponds to the Gaussian correlator (1), curve 2 to (2) with $\mu = \frac{1}{2}$, and curves 3 and 4 to (3) with $\lambda = \frac{1}{2}$ and 0. The results for conductivity are based on the formalism [11] that unites earlier approaches [12] to transport in systems with random rough walls. Elastic wall scattering leads to transitions between the states, $\epsilon_j(q) \leftrightarrow \epsilon_{j'}(q')$, with the probability $W_{jj'}(q, q')$ which is determined by the power spectrum of thickness fluctuations $\zeta(q_j - q_{j'})$ (q_j is the Fermi momentum for the miniband ϵ_j, $\epsilon_j(q_j) = \epsilon_F$):

$$W_{jj'}(q, q') = \frac{2}{m^2L^2}\zeta(q_j - q_{j'})\left(\frac{\pi j}{L}\right)^2\left(\frac{\pi j'}{L}\right)^2, \tag{5}$$

where $\zeta = \zeta_1 + \zeta_2$ is the sum of the correlation functions of inhomogeneities on the two walls, and, in order not to create parameter clutter, we assumed that the inhomogeneities from different walls are not correlated with each other. The transport equation with the scattering probabilities (5) is a set of coupled equations for the distribution functions $n_j(q)$ in each miniband ϵ_j:

$$\frac{dn_j}{dt} = 2\pi\sum_{j'}\int W_{jj'}[n_{j'} - n_j]\delta(\epsilon_{jq} - \epsilon_{j'q'})\frac{d^2q'}{(2\pi)^2}. \tag{6}$$

The structure of equations (5), (6) is the same as for scattering by impurities. For degenerate fermions, the transport equation reduces, after standard transformations, to a set of linear equations in v_j:

$$q_j/m = -\sum_{j'} v_{j'}(q_{j'})/\tau_{jj'},$$

$$\frac{2}{\tau_{jj'}} = m\sum_{j''}[\delta_{jj'}W^{(0)}_{jj''} - \delta_{j'j''}W^{(1)}_{jj'}]$$

where $n_j^{(1)} = \nu_j \delta(\epsilon - \epsilon_F) eE$ is the first angular harmonic of $n_j(\boldsymbol{q})$ at $q = q_j$, and $W_{jj'}^{(0,1)}(q_j, q_{j'})$ are the zeroth and first harmonics of $W(\boldsymbol{q}_j - \boldsymbol{q}_{j'})$ over the angle $\widehat{\boldsymbol{q}_j \boldsymbol{q}_{j'}}$. The solution of these equations provides the conductivity of the film:

$$\sigma = -\frac{e^2}{3\hbar^2} \sum_j \nu_j(q_j) q_j = \frac{e^2}{3m\hbar^2} \sum_{j,j'} \left(\frac{1}{\tau}\right)^{-1}_{jj'} q_{j'} q_j. \tag{7}$$

Instead of three length scales, L, R, and $\lambda_F = (2m\epsilon_F)^{-1/2}$, we will use three dimensionless parameters:

$$x = R/\lambda_F, \qquad y = R/L, \qquad z = L/\lambda_F. \tag{8}$$

Usually, the QSE in metal films is associated with a saw-like dependence of the conductivity σ on the film thickness L [1,6]. The oscillations correspond to abrupt changes in the number $S = \mathrm{Int}(L/\lambda_F \pi)$ of the occupied minibands ϵ_j at the points where the film thickness $L = j\pi\lambda_F$ with integer j (the Fermi wavelength $\lambda_F = 1/p_F$). These QSE oscillations exist irrespective of whether the decay of QW states is caused by bulk or surface scattering [9]. The period π/p_F of this QSE for good metals is atomic, making the observation of oscillations in $\sigma(L)$ difficult.

The drops in $\sigma(L)$ at $L = j\pi\lambda_F$ are explained by an opening of j new scattering channels for the scattering-driven transitions to and from the newly accessible highest miniband ϵ_j. The amplitude of these drops ('sawteeth') is determined by comparison of the interband transition probabilities $W_{j\neq j'}(\boldsymbol{q} - \boldsymbol{q}')$ with the intraband scattering $W_{jj}(\boldsymbol{q} - \boldsymbol{q}')$. When the off-diagonal $W_{j\neq j'}$ become small, the amplitude of the QSE decreases, reducing, eventually, the sawteeth to barely visible kinks on $\sigma(L)$ [10]. If the thickness fluctuations are the main source of scattering, the usual saw-like QSE can be observed for the inhomogeneities with small correlation radius ('size') $R < L$. For larger R the interband transitions are often suppressed, making $\sigma(L)$ smooth.

Below we demonstrate that there exists a new type of QSE oscillation at $R > L$. The new oscillations can be observed if the Fourier image $\zeta(\boldsymbol{q})$ of the correlation function of the thickness fluctuations $\zeta(\boldsymbol{s})$ (the so-called power spectrum) is rapidly going to zero at large q. This finding is illustrated in figure 1. Curves 1 and 2 for $\sigma(L)$ for correlators with exponential power spectra exhibit different types of oscillation than the usual saw-like QSE in curves 3 and 4 for the power-law spectral functions. The explanations for the new QSE and the disappearance of the usual saw-like QSE are interwoven.

The rate of decrease of $\zeta(\boldsymbol{q}_j - \boldsymbol{q}_{j'})$ at large q depends on the correlation length R via the parameters $\nu_{jj'} = R|q_j - q_{j'}|$:

$$\nu_{jj'} = \left|\sqrt{z^2 - \pi^2 j^2} - \sqrt{z^2 - \pi^2 j'^2}\right| R/L \tag{9}$$

where $z = L/\lambda_F$. The diagonal $\nu_{jj} = 0$. The faster the $W_{j\neq j'}$ go to zero with increasing $\nu_{j\neq j'}$, the earlier the usual saw-like QSE disappears.

The power spectrum of the Gaussian (1) decays at large qR as $\exp(-q^2R^2/2)$ and the off-diagonal $W_{jj'}$ go to zero faster than the diagonal ones by the factor $\exp(-\nu_{jj'}^2/2)$. For the correlators (2), (3), $W_{j\neq j'}$ go to zero as $\nu_{jj'}^{\mu-1/2} \exp(-\nu_{jj'})$. The slowest, power-law decay of the power spectrum corresponds to inhomogeneities (4). The amplitudes of the QSE drops in $\sigma(L)$ at the points $z = L/\lambda_F = k\pi$ decrease with increasing ν_{kj} at a rate that reflects the dependence $W_{kj}(\nu_{kj})$. Accordingly, the QSE saw disappears, with increasing R, first for the surfaces with Gaussian inhomogeneities, then for the correlators (2), (3), and almost never for (4). These different rates of suppression of the QSE are illustrated in figure 1 at $x = R/\lambda_F = 200$. The 2D conductivity $\sigma(L)$ is parametrized as

$$\sigma(L) = \frac{2e^2}{\hbar} \frac{R^2}{\ell^2} f_L(z, x). \tag{10}$$

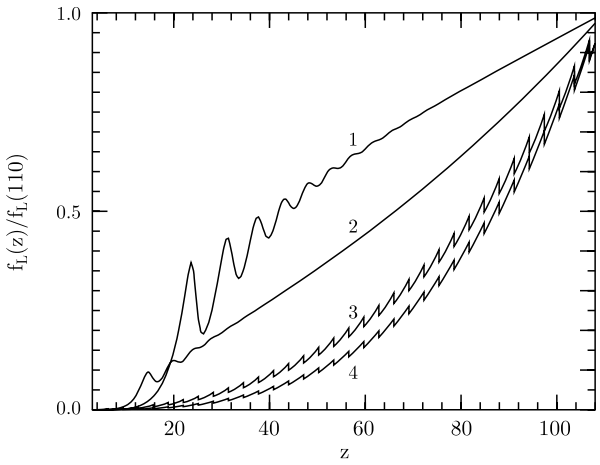

Figure 1. Normalized functions $f_L(z)$ for $\sigma(L)$ (equation (10)), $f_L(z)/f_L(z = 110)$, at $x = 200$. Curves 1 and 2 (correlators (1) and (2) with $\mu = \frac{1}{2}$; $f_L(110) = 6.9 \times 10^4$; 7.5×10^3) exhibit a new type of QSE oscillation. Curves 3, 4, for surfaces with a power spectrum (4) ($\lambda = \frac{1}{2}$; 0; $f_L(110) = 3.9 \times 10^2$; 1.3×10^1), exhibit the usual saw-like QSE.

Since $f_L(z, x = 200)$ for correlators (1)–(4) with the same values of ℓ and R have different orders of magnitude, the functions f_L, for better comparison, are normalized by their values at $z = 110$: $f_L(z)/f_L(110)$. At $x = 200$, $\exp(-\nu^2_{j\neq j'}/2)$ and $\exp(-\nu_{j\neq j'})$ are small and the QSE is suppressed for Gaussian (1) and power-law (2) ($\mu = \frac{1}{2}$) correlations (curves 1, 2), but still persists for the slowly decaying power spectra (4) with $\lambda = \frac{1}{2}$; 0 (curves 3, 4).

What is unexpected is the appearance of new large oscillations on curves 1, 2 for the Gaussian and power-law correlators. These oscillations are not related to the usual QSE, i.e., to abrupt changes in the number of occupied minibands $S(z) = \mathrm{Int}(z/\pi)$: the oscillations are less sharp, have a larger period roughly proportional to z^2, and appear only at relatively large S.

The explanation involves the interband transitions. It seems that at large R the off-diagonal $\nu_{jj'}$ (9) are large and the interband transitions are suppressed. However, for large z few of the elements $\nu_{jj'}$ with *small* j, which are close to the main diagonal, could become small even for large x; $\nu_{j,j+1}(j \ll z/\pi) \sim \pi^2 x(2j+1)/2z^2$. Then the transitions $j \leftrightarrow j+1$ could become noticeable. Analysis shows that these transition channels open when

$$W^{(0)}_{j,j+1}(x, z) \sim W^{(0)}_{jj}(x, z) - W^{(1)}_{jj}(x, z) \tag{11}$$

($W^{(0,1)}_{jj'}$ are the angular harmonics of $W(\boldsymbol{q}_j - \boldsymbol{q}_{j'})$ over the angle $\widehat{\boldsymbol{q}_j\boldsymbol{q}_{j'}}$) resulting in drops in $\sigma(L)$. Equations (11) define the positions $z_j(x)$ of such drops. At $z = z_1(x)$, W_{12} is the first of the transition probabilities to acquire the 'normal' order of magnitude. At $z = z_2(x)$, W_{23} becomes noticeable, then W_{34}, etc. The amplitudes of the drops rapidly decrease with increasing z. In the end, when many interband channels with *low* j are open, $\sigma(L)$ becomes smooth, but with a much lower slope than in its initial part. The transitions $j \leftrightarrow j+1$ with high j always remain suppressed at large x and the usual saw-like QSE does not reappear. The growth of transition probabilities for transitions $j \leftrightarrow j+2$ does not result in new oscillations in $\sigma(L)$. At the points $z(x)$ where $W_{j,j+2}$ becomes large, $W^{(0)}_{j,j+2} \sim W^{(0)}_{jj} - W^{(1)}_{jj}$, the states j and $j+2$ are already strongly coupled via $W_{j,j+1}$ and $W_{j+1,j+2}$.

A simplified, qualitative explanation of the effect and an estimate of the peak positions are as follows. Scattering by surface inhomogeneities changes the tangential momentum by $\Delta q \sim 1/R$. This is sufficient for the interband transition when this $\Delta q \sim q_j - q_{j+1}$. Since we

are interested in the minibands with a relatively small index j, $q_j^2 - q_{j+1}^2 \sim 2(q_j - q_{j+1})/\lambda_F$ (when $L/\lambda_F \gg 1$ and the index j is not large, the lateral momentum $q_j \sim 1/\lambda_F$). On the other hand, the energy conservation yields $q_j^2 - q_{j+1}^2 = \pi^2(j+1)^2/L^2 - \pi^2 j^2/L^2 \sim 2\pi^2 j/L^2$. Combining these expressions, the condition for robust interband transitions $j \leftrightarrow j+1$ can be written in the form

$$L^2 \sim \pi^2 j R \lambda_F \tag{12}$$

or, in dimensionless notation (8), $z^2 \sim \pi^2 jx$. Accordingly, with increasing L the transition channel opens first for the electrons in the lowest miniband $\epsilon_1(\boldsymbol{q})$ with $j = 1$, i.e., for the grazing electrons. Note, that these particular electrons contribute the most to the conductivity. (In the quasiclassical film without bulk scattering, the current, which is an integral over momenta, diverges when the component of momentum perpendicular to the film goes to zero, i.e., for the grazing electrons. Without the bulk scattering, the conductivity is finite only because of the quantum cut-off at $p_x = \pi/L$.) Since the electrons from the lowest miniband are responsible for the dominant contribution to the conductivity, the conductivity drops almost by half at the point $z^2 \sim \pi^2 x$ where W_{12} becomes comparable to W_{11} and the effective cross-section doubles. Let us now start increasing L. At higher values of L, $z^2 \sim 2\pi^2 x$, equation (12), a new channel opens for the electrons from the next miniband $j = 2$ with $p_x = 2\pi/L$ and the conductivity drops again, and so on. The only difference is that the contribution of the electrons from the higher minibands falls rapidly with an increase in the band index j and the drops in conductivity $\sigma(L)$, which are associated with the opening of new scattering channels for electrons from these minibands, become smaller and smaller. In some sense, the number of visible peaks in the curve $\sigma(L)$ and their relative heights give a good visual estimate of the number of 'important' minibands and of their relative contribution to conductivity. With further increase in the film thickness, when L becomes large, $L \gg R$, the change of momentum $\Delta q \sim 1/R$ is sufficient to excite *all* interband transitions and the ordinary QSE with the sawteeth at the points $z = \pi j$ is restored.

In the films with a non-exponential power spectrum of inhomogeneities, i.e., with a more uniform distribution of inhomogeneities over the sizes in momentum space, this new size effect cannot be observed because the particles from all minibands can always find inhomogeneities of the right size that ensure interband transitions irrespective of the separation between the walls.

According to [11], for Gaussian inhomogeneities

$$W_{jj'}^{(0,1)} = \frac{4\pi^5 \ell^2 R^2}{m^2 L^6} [\mathrm{e}^{-QQ'} I_{0,1}(QQ')] \mathrm{e}^{-(Q-Q')^2/2}, \tag{13}$$

($Q = q_j R$, $Q' = q_{j'} R$). The asymptotic solution of equations (11), (13):

$$z_j(x) \approx \pi \sqrt{(2j+1)x/4} \{\ln[x\sqrt{2}(1+1/j)]\}^{-1/4}. \tag{14}$$

agrees very well with the simplified estimate (12). These values $z_j(x = 200) = 24.3; 31.7; 37.7; \ldots$ agree with the positions of the peaks on curve 1 of figure 1.

For the surface with the power-law correlations of inhomogeneities (3) with $\mu \lesssim 1$, the solution of (11) is also similar to equation (12):

$$\begin{aligned} &z_j(x) = \pi \sqrt{(2j+1)x/4\nu}, \\ &\nu \sim \ln\{x(1+1/j)\sqrt{2\ln[x(1+1/j)]}\}. \end{aligned} \tag{15}$$

The saw-like drops in conductivity for the usual QSE correspond to the opening of transitions to and from the newly accessible, highest miniband while all other interband transitions are also allowed. The drops are equidistant with the period π along the z-axis,

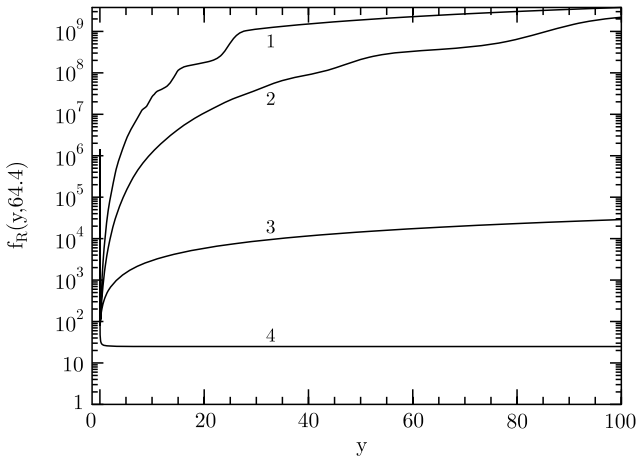

Figure 2. Functions $f_R(y)$ for $\sigma(R)$ (equation (17)), at $z = 64.4$. Curves 1 and 2 (correlators (1) and (2) with $\mu = \frac{1}{2}$) exhibit the new QSE (steps). Curves 3, 4 (correlators (4), $\lambda = \frac{1}{2}; 0$) are smooth in accordance with the usual QSE.

$z_j = \pi j$. The new QSE oscillations in figure 1 correspond to the opening of transitions between the lowest minibands, while the transitions in and out of higher minibands are suppressed. The peaks (12), (14), (15) are almost equidistant if plotted against z^2: $z_j^2 \sim \pi^2 jx$.

The initial parts of the curves 1, 2 for $\sigma(L)$ at large x are described analytically by the diagonal approximation of [11]:

$$\sigma \simeq \frac{2e^2}{3\hbar^2 m^2} \sum_j \frac{q_j^2}{W_j^{(0)} - W_j^{(1)}}. \tag{16}$$

In this range of small L, the dependence of conductivity on thickness is close to $\sigma \propto L^{(5+\alpha)}$ (small α depends on x); experimentally, the index is about 6. After the region of new QSE oscillations, the curves are again smooth, but with a smaller tangent. The numerical analysis yields either $\sigma = A + BL^{1+\beta}$ with small β or $a + bL + cL^2$, close to experimental data (see [13] and the last of references [1]) and different from the behaviour of $\sigma(L)$ at $x = p_F R \ll 1$ (see the second references in [11,12]). The dependence of the conductivity on the correlation radius of the surface inhomogeneities, $\sigma(R)$, is best illustrated by the function $f_R(y, z = \text{constant})$:

$$\sigma(R) = \frac{2e^2}{\hbar} \frac{L^2}{\ell^2} f_R(y, z = \text{constant}), \tag{17}$$

with $y = R/L$. The number of occupied minibands S does not depend on the correlation radius of inhomogeneities, and $f_R(y, z = \text{constant})$ does not have any signs of the usual QSE. Instead, the curves exhibit a step-like structure that corresponds to our new QSE of figure 1.

The positions of the singularities $y_j(z)$ for $f_R(y, z = \text{constant})$ are identified from equation (11) with $x = yz$. The functions $f_R(y, z = 64.4)$ are plotted in figure 2 for several correlators. The steps on curve 1 at the points $y = 25; 14; 8; \ldots$ agree well with the solution $y(z)$ of (14). The same feature is also observed for the power-law correlators. (Minima in all curves near the vertical axis describe the region of the most effective surface scattering at $p_F R \sim 1$.)

The dependence of the conductivity σ on the density of fermions N or their Fermi momentum p_F is best displayed by the function $f_N(z)$:

$$\sigma(p_F) = \frac{2e^2}{\hbar} \frac{L^2}{\ell^2} f_N(z, y = \text{constant}). \tag{18}$$

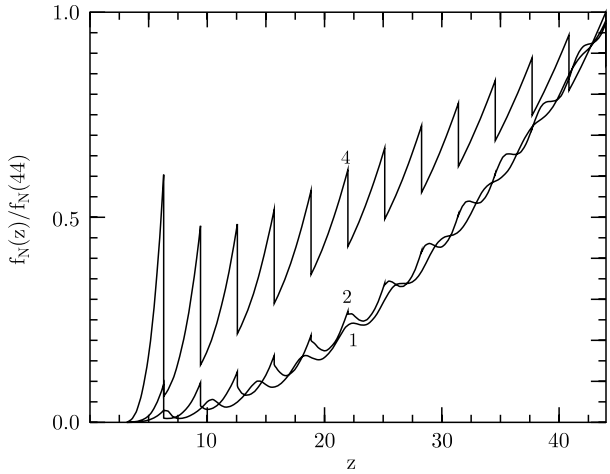

Figure 3. Normalized functions $f_N(z)$ for $\sigma(p_F)$ (equation (18)), $f_N(z)/f_N(z = 44)$, at $y = R/L = 1$. Curves 1 and 2 (correlators (1), (2) with $\mu = \frac{1}{2}$; $f_N(44) = 5 \times 10^3; 2.5 \times 10^2$) exhibit suppressed usual QSE peaks at small z that gradually transform at higher z into the new QSE oscillations with larger period. Curve 4, for surfaces with power spectrum (4) ($\lambda = 0$; $f_N(44) = 20.2$), exhibits the usual QSE.

Function $\sigma(p_F)$ exhibits the usual saw-like QSE at not very high y for all types of correlator. With increasing y, the sawteeth disappear, first for the Gaussian and later for the power-law correlators, and persist for the power-law correlators in the momentum space. Curves $f_N(z)$ exhibit the effect related to the new QSE oscillations of figure 1 for $\sigma(L)$ and to the steps in figure 2 for $\sigma(R)$. Figure 3 shows normalized (by the highest value) functions $f_N(z)$ for the correlators (1) (curve 1), (2) ($\mu = \frac{1}{2}$, curve 2), and (4) ($\lambda = \frac{1}{2}$, curve 4). The correlation radius R is small, $y = 1$, and the figure illustrates the transition from the usual to the new QSE. The correlators (4) have a slowly decaying power spectrum and the functions $f_N(z)$ reveal the usual saw-like QSE. Curve 2 starts as a usual QSE curve, but, with increasing z, the oscillations lose the saw-like shape and increase in period. Curve 1, for the Gaussian correlator with a much-faster-decaying power spectrum, does not exhibit the shape and periodicity of the usual QSE even at small z.

Curves $f_N(z)$ for the same correlators, but at $y = 20$, are shown in figure 4. Curves 3, 4 still exhibit the usual QSE, while curves 1, 2 show well-developed oscillations of the new type. The peaks on curve 1 at $z_j(y = 20) = 19.8; 50.3; 83.6; \ldots$ are described by (14) with $x = yz$.

In summary, we predict a new type of QSE in the conductivity of metal films. The effect is explained by strong coupling of low QW states caused by thickness fluctuations. The positions of the peaks (14), (15) are determined analytically. New QSE anomalies can be seen in dependencies the conductivity, the film thickness, the correlation radius of the inhomogeneities, and the particle density (Fermi momentum). These new singularities replace the usual QSE for surface inhomogeneities with large correlation radius and rapidly (exponentially) decaying power spectra such as for Gaussian or power-law correlators. Surfaces with power-law decay of the Fourier image of the correlation function exhibit the usual QSE. The effect is especially important for high-quality films with large thickness domains such as [2, 5]. The results identify the thickness fluctuations from conductivity measurements. Indices in the power-law dependence $\sigma(L)$ before and after the oscillation region agree with experiment. The large period of the new oscillations makes the observation of the QSE in metal films easier and can explain data from the third of references [1].

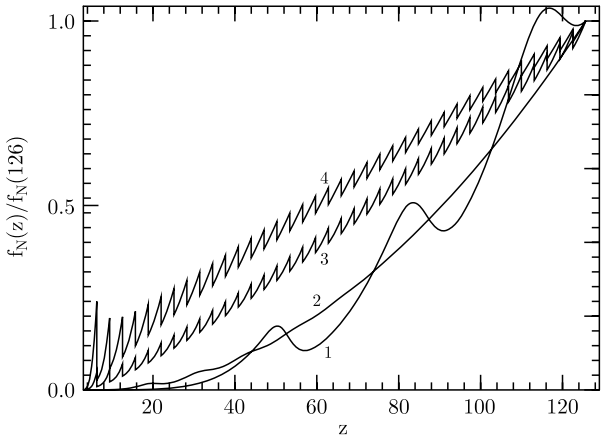

Figure 4. $f_N(z)/f_N(z = 126)$ for $y = R/L = 20$. Curves 1, 2 (correlators (1) and (2), $\mu = \frac{1}{2}$; $f_N(126) = 1.1 \times 10^9$; 4.5×10^7) exhibit well-developed new QSE oscillations. Curves 3, 4, for correlators (4) with $\lambda = \frac{1}{2}$; 0 ($f_N(126) = 1.4 \times 10^4$; 47). still exhibit the usual saw-like QSE.

An important issue for direct observation of the new QSE is the experimental possibility of producing films of different thicknesses, but with the same correlation function of the surface inhomogeneities. The important point, which can make this possible, is that the only interesting situation is when the size of the inhomogeneities R is larger than the film thickness. There are several options:

(i) One can grow a crystal film at a given angle to the crystalline axes.
(ii) In the case of film deposition, the deposition can be properly manipulated on a relatively large scale R.
(iii) One can prepare a film with 'perfect' surfaces and introduce large-scale inhomogeneities later.

The underlying high sensitivity of the coupling of low QW states to the type and parameters of the thickness fluctuations is quite general and can also lead to visible effects for grazing electrons in semiconductor films and quantum waveguides such as in [14]. More detailed results will be published elsewhere [15].

Acknowledgment

The work was supported by NSF grant DMR-0077266.

References

[1] Jalohowski M, Hoffman H and Bauer E 1996 *Phys. Rev. Lett.* **76** 4227
Kuzik L A, Petrov Yu E, Pudonin F A and Yakovlev V A 1994 *Sov. Phys.–JETP* **78** 114
Mikhailov G M, Malikov I V and Chernykh A V 1997 *JETP Lett.* **66** 725
[2] Paggel J J, Miller T and Chang T C 1999 *Science* **283** 1709
Evans D A, Alonso M, Cimino R and Horn K 1993 *Phys. Rev. Lett.* **70** 3483
[3] Andreieu S, Chatelain C, Lemine M, Berche B and Bauer Ph 2001 *Phys. Rev. Lett.* **86** 3883
[4] Altfeder I B, Chen D M and Matveev K A 1998 *Phys. Rev. Lett.* **80** 4895
Altfeder I B, Chen D M and Matveev K A 1997 *Phys. Rev. Lett.* **78** 2815
[5] Paggel J J, Miller T and Chang T C 1998 *Phys. Rev. Lett.* **81** 5632
Patthey F and Schneider W-D 1994 *Phys. Rev.* B **50** 17 560

Schmid M, Hebenstreit W, Varga P and Crampin S 1996 *Phys. Rev. Lett.* **76** 2298
[6] Jalohowski M, Bauer E, Knoppe H and Lilienkamp G 1992 *Phys. Rev.* B **45** 13 607
Jalohowski M, Hoffman H and Bauer E 1995 *Phys. Rev.* B **51** 7231
[7] Ogilvy J A 1991 *Theory of Wave Scattering from Random Surfaces* (Bristol: Adam Hilger)
Feenstra R M, Collins D A, Ting D Z-Y, Wang M W and McGill T C 1994 *Phys. Rev. Lett.* **72** 2749
[8] Palasantzas G and Barnas J 1997 *Phys. Rev.* B **56** 7726
Palasantzas G, Zhao Y-P, Wang G-C, Lu T-M, Barnas J and De Hosson J Th M 2000 *Phys. Rev.* B **61** 11 109
[9] Sandomirskii V B 1968 *Zh. Eksp. Teor. Fiz.* **52** 158 (Engl. transl. 1967 *Sov. Phys.–JETP* **25** 101)
Trivedi N and Ashcroft N W 1988 *Phys. Rev.* B **38** 12 298
[10] Meyerovich A E and Stepaniants S 1997 *J. Phys.: Condens. Matter* **9** 4157
[11] Meyerovich A E and Stepaniants A 1998 *Phys. Rev.* B **58** 13 242
Meyerovich A E and Stepaniants A 1999 *Phys. Rev.* B **60** 9129
Meyerovich A E and Stepaniants A 2000 *J. Phys.: Condens. Matter* **12** 5575
[12] Tesanovic Z, Jaric M V and Maekawa S 1986 *Phys. Rev. Lett.* **57** 2760
Fishman G and Calecki D 1989 *Phys. Rev. Lett.* **62** 1302
Kawabata A 1993 *J. Phys. Soc. Japan* **62** 3988
Meyerovich A E and Stepaniants S 1994 *Phys. Rev. Lett.* **73** 316
Meyerovich A E and Stepaniants S 1995 *Phys. Rev.* B **51** 17 116
Makarov N M, Moroz A V and Yampol'skii V A 1995 *Phys. Rev.* B **52** 6087
[13] Henz J, von Känel H, Ospelt M and Wachter P 1987 *Surf. Sci.* **189–90** 1055
Duboz J Y, Badoz P A, Rosencher E, Henz J, Ospelt M, von Känel H and Briggs A 1988 *Appl. Phys. Lett.* **53** 788
[14] Sanchez-Gill J A, Freilikher V, Yurkevich I and Maradudin A A 1998 *Phys. Rev. Lett.* **80** 948
[15] Meyerovich A E and Ponomarev I V 2002 *Phys. Rev.* B **65** at press